Root-induced changes in the hydraulic properties of a fine slope cover

Vito Tagarelli[1#], *Nico* Stasi[2], *Federica* Cotecchia[1], *Francesco* Cafaro[1]

[1]*Polytechnic University of Bari, DICATECh, Via Orabona 4, Bari, Italy*
[2]*University of Bari, Piazza Umberto I 1, Bari, Italy*
[#]*Corresponding author: vito.tagarelli@poliba.it*

ABSTRACT

Recently, the soil-vegetation-atmosphere (SVA) interaction is becoming a topic of intense scientific research within the geotechnical community, because it was recognized to potentially induce significant pore pressure variations in slopes, at both shallow and larger depths, being then responsible for weather-induced landsliding.
The processes within such interaction are of different nature, and result in a chemo-thermo-hydro-mechanical transient boundary condition at the ground level, causing exchanges of liquid, gas and energy within the soil cover layer (from ground level to 3-4 metres depths). Hence, both the soil cover material and its thermo-hydro-mechanical constitutive properties, as well as the vegetation properties, become of key relevance within such processes.
In this study, with reference to a full scale in-situ test where deep-rooted crop spices were seeded and farmed, the hydraulic properties of rooted clayey soil were investigated in the laboratory as well as in-situ in terms of both saturated permeability and retention properties. As for the saturated permeability, both laboratory and in-situ tests were conducted, the latter being also back-analysed. The retention states of the material were investigated by means of the filter paper technique in the laboratory and were of use for the numerical back-analyses of the Guelph-induced wetting process in the soil cover.
The measurements show that roots within the vegetated zone determine both an increase of the permeability and a reduction of the retention properties of the composite material if compared to the soil in bare conditions.

Keywords: Saturated permeability; Guelph permeameter; rooted soil; deep-rooted vegetation; numerical analyses.

1. Introduction

The recent scientific literature shows an increase of the geotechnical research activity concerning the experimental study of the soil-vegetation-atmosphere (SVA) interaction (*e.g.,* Blight, 1997; Leroueil, 2001; Gens, 2010; Toll *et al.,* 2011; Smethurst *et al.,* 2015), which controls the conditions at the ground surface of geotechnical systems. With reference to slopes, the SVA interaction has been shown to impact the variations with time of the pore water pressures, either at shallow or large depths, even within clay slopes, and as such, to control landslide activity (Cotecchia *et al.*, 2014; 2015; Pirone *et al.* 2015). The cause-effect relationship between the activity of landslides and the SVA interaction has been characterized not only through field monitoring but also through numerical modelling (Cotecchia *et al.,* 2014; Tagarelli and Cotecchia 2019; 2020; Pedone *et al.,* 2021; di Lernia *et al.,* 2022).

Several processes of different nature are involved in the SVA interaction and together determine the thermo-hydro-mechanical transient top boundary of the slope. They occur within the first 3-4 metres depth, where the gradients controlling the liquid, gas, and energy exchanges between the soils and both the atmosphere and the vegetation are maximum. Hence, the thermo-hydro-mechanical constitutive properties of the rooted soil by this depth, together with the vegetation properties, are of key relevance in the assessment of the slope scale thermo-hydro-mechanical balances that influence the slope stability (Elia *et al.,* 2017; Cotecchia *et al.,* 2019; Pedone *et al.,* 2021).

This paper is intended to contribute to the characterization of the permeability function of the top layers of soil deposits, performing experimental tests on the topsoils covering a clayey slope. The results of the study are in turn intended to allow for advancement in the modelling of the SVA interaction.

Field and laboratory tests were carried out to characterize the permeability function of a heterogeneous clayey soil cover that outcrops in the toe area of an active slow-moving landslide in the southern Apennines, the Pisciolo landslide (Italy; Cotecchia *et al.,* 2014). The field tests were performed within portions of the soil cover rooted by spare wild vegetation, referred to as bare in the following, and portions referred to as vegetated cover, where selected deep-rooted species had been seeded and farmed. The selected vegetation species had been seeded in order to investigate the effects of different vegetation typologies on the SVA interaction at the ground surface of the slope and, hence, on the corresponding water infiltration rates that affect the slope stability (Tagarelli and Cotecchia 2022).

The test results discussed in this paper contribute to innovate the strategy to characterize the permeability function of composite soil covers, made of soil and roots, and also provide evidence of the dependence of the hydraulic properties of clayey soil on the vegetation

and root network typology. The assessment of the field permeability function is based on a finite element numerical back-analysis of in-situ Guelph tests, implementing the soil water retention properties. The field value of the saturated permeability is compared with that resulting from laboratory testing.

2. Sampling site and testing methods

Extensive field and laboratory investigation campaigns were carried out in the past to characterize the geo-hydro-mechanical behaviour of the clayey soils (clay fraction, CF: 20%<CF<60%) present down to large depth in the Pisciolo slope, as reported by Cotecchia *et al.,* (2014; 2019) and Pedone *et al.,* (2021).

The tested clayey soil covers the toe area of the Pisciolo slope (Tagarelli & Cotecchia 2022, Assadi-Langroudi *et al.,* 2022) where an area of 2000 m^2, was partly seeded with selected deep-rooted Gramineae plants. Both the selection of the species and their seeding were carried out by the Italian company "PratiArmati s.r.l.", through an innovative green technology, previously adopted to mitigate rainfall-induced erosion (Apollonio *et al.,* 2021). The hydraulic characterization of the clayey soil cover, either vegetated, or bare, entailed the measurement of the related values of saturated permeability, k_{sat}, both in-situ and in the laboratory. Both rooted and bare soil samples were collected in situ for the laboratory testing, by using a manual auger (50-56mm diameter, 50 mm height).

2.1. Laboratory testing

As anticipated, the laboratory characterization was carried out by testing samples collected in-situ within the soil cover (0-0.5m depth), either inside (V in the following) or outside (in the bare area, B in the following) the vegetated area.

The soil composition was characterized through the soil grading and the index properties, whereas the soil state was characterized in terms of: natural water content, w_n, void ratio, e, unit weight, γ, degree of saturation, S_r, and suction, s, on the undisturbed samples. In particular, e and S_r were determined in the laboratory by measuring the volume of the specimens, as well as both the gravimetric water content and the specific gravity of solids, G_s. It is believed that the shrinkage of the roots may have caused γ_{dry} to be underestimated, and e to be overestimated, but only to a minor extent, since the roots weight and volume can be assumed negligible compared to those of the samples.

Tests in the laboratory were carried out on undisturbed samples for the determination of the coefficient of saturated permeability, k_{sat}. To this aim specimens of 56 mm diameter and 20 mm height were trimmed and subjected to constant head permeability tests in a modified permeameter (Bottiglieri *et al.,* 2012), which allows for the direct measurement of the vertical k_{sat} for the soil subjected to an imposed vertical effective stress while in oedometric conditions.

The retention states, describing the partially saturated soil behaviour, were measured in the laboratory by determining the water content, ϑ_w, and the suction, s, of specimens trimmed from the undisturbed samples (56 mm diameter and 20 mm height); s was measured by means of the filter paper technique, using the Whatman No. 42 filter paper (matrix suction, s; Marinho and Oliveira 2006). Hence, the van Genuchten fitting model (van Genuchten, 1980) was used for determining the soil water retention curves (SWRC).

Moreover, determinations of root density in the soil specimens were carried out. In particular, after the determination of both the k_{sat}, and the WRCs, roots were separated and then detached from the soil specimens in the laboratory by hand sieving (Benjamin *et al.,* 2004) by adopting a #40 (ASTM standard) mesh stainless steel. The resulting root pieces from each specimen were scanned and then subjected to digital image analyses by means of the code RhizoVision Explorer (Seethepalli *et al.,* 2021) to quantify the length and diameter of the roots present in each specimen. Finally, the root length density (*RDL*) was calculated as the root length per soil volume of each soil specimen.

2.2. In-situ testing

Field k_{sat} determinations of the soil cover were carried out using the Guelph permeameter (Soilmoisture Equipment Corp., 2008) in May 2021 and in March 2022, for B and V conditions.

The Guelph's test procedure prescribes the application of a water flow to recharge a 30 cm depth cylindrical well drilled through the soil cover, in order to keep a constant water head in the well during the whole test. The flow rate corresponding to the reach of a steady state seepage through the well surface is used to compute k_{sat} according to the Guelph-Richards procedure reported by Reynolds *et al.,* (1985). The values of k_{sat} were computed using the single-head approach by Elrick *et al.*, (1989), who provided a closed-form solution of the seepage problem:

$$k_{sat} = \frac{cQ}{2\pi H^2 + C\pi r^2 + 2\pi \frac{H}{\alpha^*}} \quad (1)$$

where, H is the imposed constant water head, r is the radius of the well hole, C is a shape parameter function of both H and r, and Q is the flow of water necessary to keep the constant water head in the well, and α^* is a macroscopic capillary length parameter. Eq. (1) was used to derive k_{sat} for each of the Guelph tests carried out at Pisciolo, where a water head h_1=15cm was imposed for about three hours for tests 1 and 2 within the vegetated area (V) and for test 1 within the bare area (B); whereas, as for the test 2 within B, a constant water head h_2=25cm was imposed for about two hours.

For each Guelph test, one undisturbed soil sample was collected during the excavation of the well hole, later subjected to soil state determination in the laboratory, in terms of void ratio, e, degree of saturation, S_r, and matrix suction, s. The same determinations were also conducted in the laboratory on samples collected at the end of each Guelph test, collected by further deepening inside the well hole, aimed at measuring the final soil state. Such determinations were of reference for performing the numerical back-analyses of the Guelph test data, used to simulate more realistically the

seepage induced during the field test and estimate accurately the k_{sat} of the soil cover.

2.3. Numerical back-analysis

The Guelph-induced transient seepage in the soil cover during the test was back-analysed through fully coupled hydro-mechanical numerical analyses using the FE code PLAXIS 2D with the aim to assess the isotropic k_{sat} value at the field scale. The FE code Plaxis 2D (Bentley, 2022) implements Biot's theory (Biot, 1941) to model the transient seepage through the soil, accounting for partial saturation and hydro-mechanical coupling (Galavi, 2010). An homogeneous and isotropic soil was considered, whose mechanical behaviour was modelled with the elastoplastic Mohr-Coulomb constitutive model, accounting for the partially saturated soil condition modelled according to the single stress variable framework (Bishop, 1959) and by using the Mualem-van Genuchten model (Mualem, 1976; van Genuchten, 1980) for the soil water retention curve, whose parameters were fitted (van Genuchten *et al.,* 1992) based upon the laboratory data during drying-wetting retention tests on the undisturbed specimens taken in either the vegetated (V) or the bare (B) area. Table 1 reports the fitted parameters together with strength and stiffness parameters adopted.

Table 1. Hydro-mechanical parameters implemented in the numerical back-analyses.

	Vegetated (V)	Bare (B)
S_{sat} [-]	1	1
S_{res} [-]	0.13	0.13
g_a [1/m]	0.0541	0.067
g_n [-]	1.346	1.201
E' [kN/m^2]	10710	10710
ν' [-]	0.3	0.3
φ' [°]	18	18
c' [kN/m^2]	5	5
Ψ [°]	0	0

The formulation just reported was already adopted and yielded successful numerical predictions for SVA interaction modelling (Tagarelli & Cotecchia 2020) as well as for the modelling of drainage-induced water seepage in the slope (Tagarelli & Cotecchia 2022).

Since the analyses were performed to evaluate the k_{sat} value at the field scale for all the Guelph tests, for each of them, a set of parametric analyses for varying k_{sat} values were run, simulating the infiltration occurred during the test, for the exact time duration of the specific test. It was then selected as correct the k_{sat} value corresponding to the simulation in which the water volume infiltrated through the well hole during the whole test duration was equal to that measured in situ.

The finite element mesh for axial-symmetrical analysis (1m*1m wide) implemented the axial symmetrical well with a radius of 3cm and a depth of 30cm. The right and bottom boundary conditions were set both far away so not to influence the simulated transient water flow in the soil. The initial total stress state in the model was defined by applying the k_0-procedure, consistently with what reported by Tagarelli & Cotecchia (2020), adopting a $k_{0,initial}$=1; instead, the pore water pressure regime was computed by using the head boundary condition type; in particular, a steady state seepage state was computed with the vertical lateral boundaries as impervious, while a constant total head was applied at the top and bottom boundaries causing a constant suction value within the model, consistent with the initial value monitored at the beginning of the in-situ test.

After the initialization of the effective stresses, the excavation of the well hole was modelled by deleting the corresponding soil cluster in the FE model; furthermore, within the same calculation phase the transient water flow was also applied, by activating a constant pressure head boundary condition; in particular, a total head condition was applied at the boundaries inside the well hole in the numerical model consistent with the constant water level acting in the well during the Guelph test. Impervious hydraulic boundary conditions were set to the right, left and bottom sides for the whole transient phase of the numerical analysis, whereas the upper boundary condition was set as free drainage.

The numerical back-analyses were performed for both the Guelph tests carried out in May 2021 and March 2022 (Test 1 and Test 2 in Table 2, respectively), either in the vegetated (V) or in the bare (B) area. The corresponding initial states, in terms of void ratio, e, suction, s, degree of saturation, S_r, are reported in Table 2 and discussed in the next paragraphs.

It is worth mentioning that the comparison between the in-situ and laboratory k_{sat} may be not very well posed, since the first better represents the in-situ condition (*e.g.,* anisotropy of the soil-root composite), whereas the second is more representative of an imposed vertical water seepage in the soil specimen.

Table 2. Physical properties and initial state of the soil sampled inside and outside the vegetated area at the beginning of the Guelph's permeability tests.

	Vegetated (V)		Bare (B)	
	Test 1	Test 2	Test 1	Test 2
Clay fraction, CF [%]	14.9	17.4	12.2	11.1
Silt fraction MF [%]	31.22	38.7	48.4	44.6
Sand fraction SF [%]	53.8	43.9	39.4	44.3
Dry unit weight, γ_{dry} [kN/m^3]	15.6	14.9	14.5	15.4
Natural water content, w_n [%]	17.9	22.8	29.5	26.1
Void ratio, e [-]	0.71	0.78	0.83	0.82
Degree of saturation, S_r [%]	68.5	78.7	95.8	97.6
Suction, s [kPa]	589	532	106	78

3. Results and discussion

3.1. Soil physical properties and initial state

Table 2 reports the results of the grading determinations on the undisturbed samples, V and B, collected before the Guelph tests 1 and 2, which on the

whole show very similar soil fractions. However, the V samples are found to be slightly more sandy and less silty than the B samples, although to a minor extent. Such difference falls in the relevant lithological variability across the soil cover and suggests that changes in either the retention properties or the k_{sat} of the soil cover may be due to differences in soil fractions only to a minor extent.

The plasticity index of the material in the cover is about 42%, whereas the activity is about 0.72, consistently with what reported in the literature also for deeper soil specimen at Pisciolo (Cotecchia *et al.,* 2014).

Six samples collected from either the V or the B area were subjected to the root analysis, according to the procedure in section 2.1, allowing for the determination of the *RDL*. As example, Figure 1 reports a picture of the undisturbed samples, V and B, subjected to root analyses (Figure 1a), along with the corresponding roots retrieved from the samples and scanned (Figure 1b).

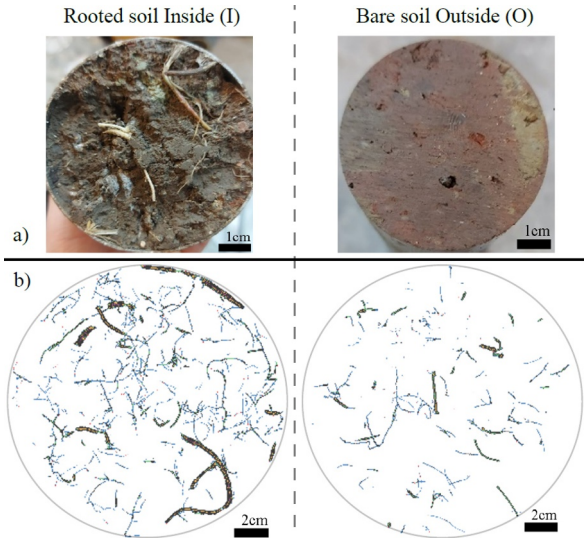

Figure 1. Photos of undisturbed samples retrieved in May 2021 (a) and corresponding scanned root image (b); V sample on the left-hand side and B sample on right-hand side.

The *RDL* of the V samples (*i.e.,* V Test 1, and V Test 2) varies in the range 3.2÷3.4 cm*cm^{-3}, whereas its value is between 1.1÷1.6 cm*cm^{-3} for the B samples (*i.e.,* B Test 1, and B Test 2), which are still values typical for grass vegetation species (Lu *et al.,* 2020). The digital image analyses also show that most of the diameters of the roots are in the range 0.5-1mm, although root diameters lower than 0.5mm were also found. Larger root diameters, *i.e.,* ranging between 1-2mm and above, were found mainly in the V samples.

The impact that roots may have on the soil state, is not a matter fully clarified in the scientific literature, since the root-induced soil modifications depend on the soil type and state, as well as both the type and stage of growth of the vegetation, as reported in the review paper by Lu *et al.,* (2020). Figure 2 reports data of both the B and V tested specimens in terms of S_r, w_{nat}, s, ϑ_{sat}, n, and γ_{dry}, with reference to the corresponding *RDL* values obtained within this research.

As for the initial state, the V specimens were found with suction values of about 550 kPa and S_r values of about 70%, whereas the B specimens were characterized by lower suction values, *i.e.,* about 100 kPa, and S_r values higher than 95% (Figure 2a and c, Table 2); accordingly, the w_{nat} was found to be lower for higher *RDL* values (V samples, Figure 2b), even though the w_{nat} values may be overestimated only to a negligible extent, due to the root shrinkage associated with the loss of water during the measurements.

Table 2 also reports the initial void ratio of all the specimens, which resulted to be coherent with the s and S_r determinations discussed above.

Furthermore, the roots appear to cause in the specimens no appreciable differences in the volumetric water content values in the final state (*i.e.,* saturated conditions, Figure 2d), as for the porosity, n. No relevant differences in the γ_{dry} were identified (Figure 2e), coherently with what was first assumed in section 2.1, due to the negligible total weight and volume of the roots in the specimen if compared to the total weight and volume of the specimen itself.

It is worthty to note that w for the saturated V and B specimens was found to be not strongly affected by increasing *RDL* values (Figure 2b), consistently with the corresponding porosity values (Figure 2d).

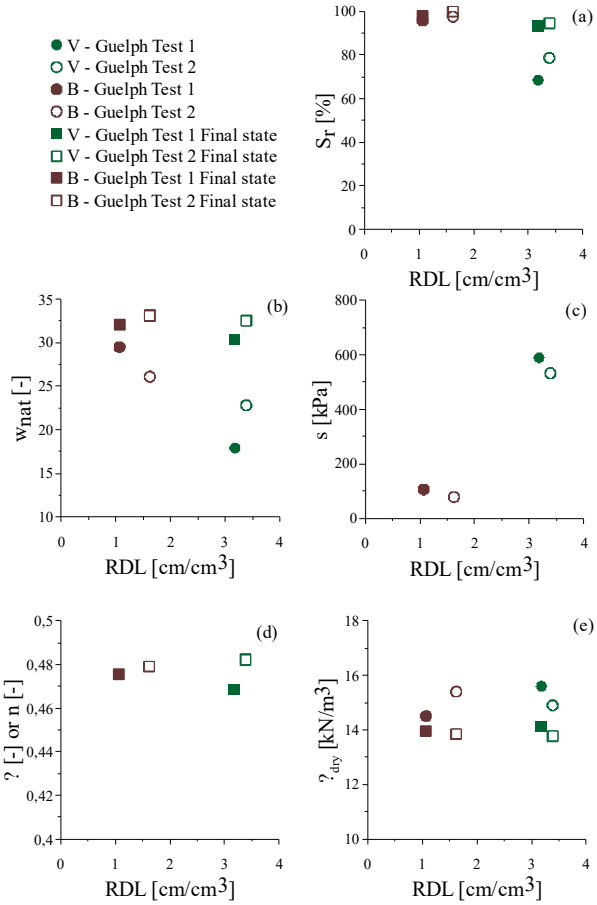

Figure 2. Soil properties, *e.g.,* ϑ_{sat}, n, γ_{dry}, and soil state, *e.g.,* w_{nat}, S_r, and s, for the tested B and V samples.

3.2. Soil water retention properties

Soil retention states along drying and wetting paths were monitored in the laboratory with reference to both V samples (green dots in Figure 3), and B samples (brown dots in Figure 3). The Figure also reports the

fitting water retention curves, WRCs, shown with green (V) and brown (B) lines, obtained through the RETC Code Vers. 6.02 (M. Genuchten *et al.,* 1992). These fitting functions, whose parameter are in Table 1, were defined so as to match better the wetting ϑ_w-s states (empty symbols in Figure 3), rather than those relating to drying (full symbols in Figure 3), since the WRC had to be implemented in the back-analyses of the Guelph-induced wetting process.

The ϑ_w-s data reported in Figure 3 provide clear evidence to the decrease in retention capacity determined by the root quantity increase within the V soil. It is recorded that the root system slightly reduces the air entry value, AEV, of the soil-root composite, when compared with that of the bare soil. Furthermore, the WRC of the rooted soil is found to be slightly steeper than that of the bare soil. It is worthy to remind that this occurs despite the B samples were found even slightly coarser that the V samples, testifying that the roots may impact relevantly on the soil water retention properties.

On the whole, the recorded impact of the root system on the ϑ_w-s retention curve of the soil-root composite recorded in the laboratory is fully consistent with that observed in other studies on both fine and coarser soils as reported in the literature by Lu *et al.,* (2020).

The roots make the fine material less retentive than the undisturbed one (*i.e.*, B), by possibly modifying its meso-structure through a mechanism of amalgamation of micro-aggregates (2–250 μm) by increasing macro-pore volumes as recognized likely to happen in several cases by (Lu *et al.*, 2020).

It is also worth noting that the retention data of the B soil here reported are found to be fully consistent with retention states monitored and reported already in the literature for the Pisciolo clay by Cotecchia *et al.,* (2014) and Pedone *et al.,* (2022).

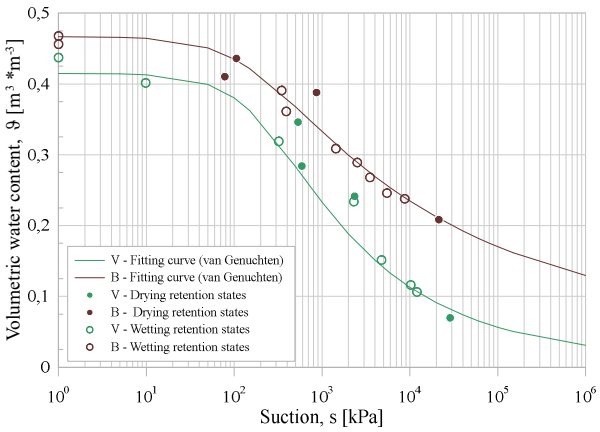

Figure 3. Soil-water retention states (ϑ_w-s) for both the vegetated (V, green dots) and bare (B, brown dots) specimens for both drying and wetting paths and corresponding fitting WRC (green line for V, brown line for B).

3.3. Saturated permeability

The tests conducted in the laboratory by means of the modified permeameter allowed for the measurement of k_{sat} for either V or B samples. The measured k_{sat} values are $1.40*10^{-09}$ m/s and $1.20*10^{-07}$ m/s for the bare soil (B) and the vegetated soil (V), respectively (Table 3).

The field value of k_{sat} derived using Eq. (1), (Reynolds *et al.,* 1985) ranges, from $4.5*10^{-09}$ m/s to $3.9*10^{-09}$ m/s between May 2021 (Test 1) and March 2022 (Test 2) in the bare area (B); in the vegetated area (V), instead, k_{sat} according to Eq. (1) is found to be about constant, $7.4*10^{-08}$ m/s - $5.9*10^{-08}$ m/s between Test 1 and Test 2 (Table 3). However, as anticipated, the field values of k_{sat} were also derived through numerical back-analyses of the Guelph's induced water seepage from the well hole; in particular, the initial soil state data (*i.e.,* void ratio, suction and degree of saturation) were of use to inform the initialization phase of the FE numerical modelling. Accordingly, given the similarity of the initial in-situ state values s - S_r (Table 2) for both tests in either the V or the B area, in the initialization phase of either tests s=550 kPa and S_r=70% were imposed to be uniform in the V area, whereas s=100 kPa and S_r=97% were imposed to initialize the numerical model in the B area.

Subsequently, the Guelph-induced transient seepage was activated by setting the hydraulic boundary conditions to be consistent with a water table of 15 cm above the bottom of the hole for both Test 1 and Test 2 in the V area and for Test 1 in the B area, whereas the water table was set equal to 25 cm above the bottom of the hole for Test 2 in the B area. During the transient seepage phase, the volume of water flowing with time through the submerged boundary was computed till the reach of the total in-situ testing time. The analysis was repeated for different values of k_{sat} and the value corresponding to a computed total volume of water infiltrated equal to that measured in-situ was selected as back-analysed field k_{sat}.

Table 3. Values of the coefficient of the saturated permeability determined with reference to in-situ and laboratory testing, as well as obtained from numerical back analyses, for the vegetated (V) and bare (B) areas.

	Vegetated (V)	**Bare (B)**
Test 1 (Eq. (1))	$7.4*10^{-08}$ [m/s]	$4.5*10^{-09}$ [m/s]
Test 2 (Eq. (1))	$5.9*10^{-08}$ [m/s]	$3.9*10^{-09}$ [m/s]
Laboratory testing	$1.2*10^{-07}$ [m/s]	$1.4*10^{-09}$ [m/s]
Test 1 (Back-analysis)	$3*10^{-09}$ [m/s]	$6*10^{-10}$ [m/s]
Test 2 (Back-analysis)	$1.3*10^{-09}$ [m/s]	$3*10^{-10}$ [m/s]

Figures 4a and 4b report, for both the V and the B area, the measured cumulated water volume (cm^3) flowed with time through the submerged Guelph permeameter hole (*i.e.,* full and empty dots for Test 1 and Test 2, respectively), compared with the corresponding computed volumes (*i.e.,* continuous and dashed black lines for Test 1 and Test 2, respectively) from the numerical back-analyses.

By making reference to the water volume lost within the Guelph tests (Figures 4a and 4b), it is evident that the volume discharged in the V area was far higher (about one order of magnitude) than that discharged in both the tests in the B area, being a clear indication of a higher permeability of the V soil cover.

For all tests the k_{sat} values resulting from the numerical back-analyses are lower than those calculated

from in-situ tests, through Eq. (1), in Table 3. In particular, in the V area k_{sat} resulting from the back-analysis of Test 1 is $3*10^{-09}$ m/s, lower than that calculated by Eq. (1), $7.4*10^{-08}$ m/s, whereas for Test 2 the numerical k_{sat} is $1.3*10^{-09}$ m/s, lower than $5.9*10^{-08}$ from Eq. (1). In the B area, the back-analysed k_{sat} value is $6*10^{-10}$ m/s for Test 1, instead of $5*10^{-9}$ m/s, as well as for Test 2 the back-analysed k_{sat} is $3*10^{-10}$ m/s against $4*10^{-9}$ m/s.

It is long since well-known (*e.g.,* Chapuis, 1989; Avci 1994; Chandler *et al.,* 2015) that the shape factor in Eq. (1), which has to be assumed, is of key relevance in the k_{sat} estimate; the results commented here give evidence to the size of error that the current assumption determines, since it can be assessed that the numerical back analyses discussed above reproduce the seepage process occurring during the Guelph test rather accurately; the only possible source of uncertainty of this modelling would lie in the Mualem model used to simulate the hydraulic function when the soil is partially saturated. However, the closeness of the measured water volume versus time curves in Figures 4a and 4b to the corresponding computed curves suggests that such uncertainty does not significantly affect the numerical predictions and may represent a source of minor error within the numerical procedure to determine k_{sat} from the Guelph test data, herewith proposed.

Figures 4a and 4b also report the water discharge with time predicted by the numerical model when adopting for all the tests the k_{sat} values derived from in situ tests, Eq. (1). The predicted curves (brown continuous and dashed lines for B1 and B2, and green continuous and dashed lines for V1 and V2) are far higher than those recorded in-situ. Such comparison gives further evidence to the overestimation of water infiltration that the use of Eq. (1) to estimates the k_{sat} of a soil cover may determine.

The k_{sat} laboratory determination is found to strongly overestimate the vegetated soil cover permeability derived from the numerical back-analysis of the field test, whereas such overestimate is minor for the bare soil cover (Table 3). Indeed, the back-analysed field value of k_{sat} in the V area is lower than the laboratory one of a factor of 65 in average, whereas this difference becomes of a factor of about 3 on average, for the B area. The difference among the in-situ and laboratory k_{sat} determinations is well known in the literature since long time (*e.g.,* Childs *et al.,* 1957), and it is usually related to the different volumes involved in the seepage process; indeed, when dealing with the hydraulic characterization of heterogenous soil deposits as in this case, the representative elementary volume (REV) is expected to become larger than what would be in an homogeneous soil, possibly even larger than the REV usually tested in the laboratory. However, the larger difference occurring between laboratory and in-situ (back-analysed) determinations for the V tested samples compared to the B one, may be attributed to the presence of roots, *i.e.,* higher *RDL* values.

Furthermore, as for the V specimen tested in the laboratory, the k_{sat} value is possibly also influenced by the decaying process that some roots may have undergone (*i.e.,* loss of turgidity) before testing in the laboratory; this would provide an overall increase in the void ratio, which may justify the higher k_{sat} value measured in the laboratory. Accordingly, a few studies in the literature (Wu *et al.,* 2020; Cui *et al.,* 2022) support the hypothesis that the root decay may give rise to preferential flow paths, increasing the overall value of k_{sat}. However, such results highlight that a scale dependency may apply to the k_{sat} determinations in the laboratory, especially when high *RDL* values occur, since the k_{sat} value for the V sample (*i.e.,* full green rhombus) and the Guelph's back-analysed k_{sat} values were found to differ of almost 2 orders of magnitude (*i.e.,* V Test 2), whereas, this distance strongly decreases for the B specimens. Such difference is expected to be due to the root content in the laboratory specimen for the permeameter testing, which hence, poses a REV issue. The dimension of the REV is expected to increase proportionally with both the size and number of roots and so with the *RDL*, as reported in the literature by Shackelford *et al.,* (1991) and Fraccica & Romero (2019). As such, the k_{sat} determinations in the laboratory herein reported, since carried out with reference to standard sample dimensions (*i.e.,* oedometer soil sample, 56x20 mm) are possibly misestimated.

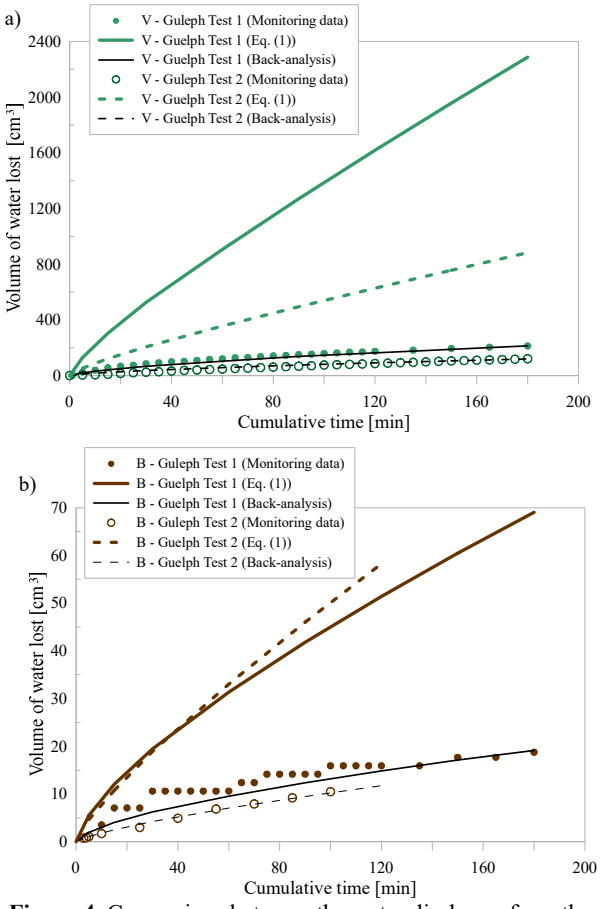

Figure 4. Comparison between the water discharge from the numerical simulation and the in-situ measurements, for tests in V area (plot a) and in B area (plot b), together with the numerical predictions with k_{sat} values from Eq. (1).

Figure 5 reports all the obtained k_{sat} values with the *RDL* values. Similarly, to what reported by Vergani *et al.,* (2016), it is possible to deduce a relation between k_{sat} and *RDL* for the k_{sat} values resulting from the numerical back-analysis of the field tests. As expected,

k_{sat} of the rooted soil increases with increasing *RDL*, following the function reported in Figure 5.

It is worthy to mention that the curve in Figure 5 does not hold the ambition to represent a general relation between the *RDL* and the k_{sat} of the soil-root composite, but rather, it is clear evidence of the impact that roots may have on the hydraulic behaviour of a fine soil cover.

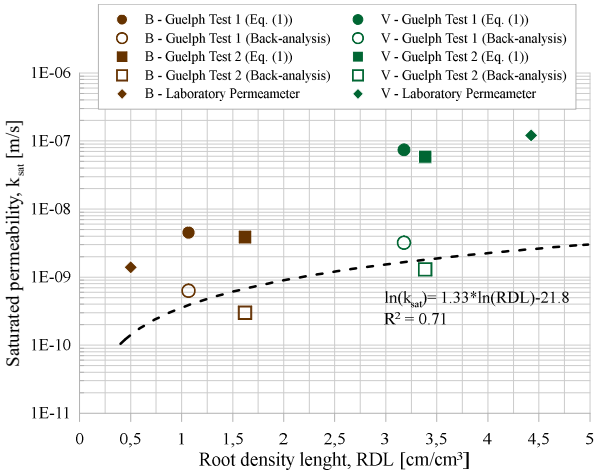

Figure 5. Results of the k_{sat} determinations via Eq. (1) (dots for the Test 1 and squares for the Test 2), via laboratory permeameter (rhombuses), and via numerical back-analysis (empty dots for the Test 1 and empty squares for the Test 2) plotted against the corresponding values of the *RDL*.

4. Conclusion

The research activity here reported was aimed to provide a contribution in addressing the open issue of the impact the root system may have on the hydro-mechanical properties of the soil-roots composite; indeed, deepening the knowledge on such impact is believed to be highly useful for researchers willing to model processes involving both soil and vegetation (*e.g.,* SVA interaction).

Despite this research activity provides only few data, it was recognized that the impact of the hydro-mechanical properties of the soil root composite may be relevant with peculiar reference to the coefficient of saturated permeability, k_{sat}, and the soil water retention curve, SWRC. It was found that the retention properties of the rooted soil were decreased if compared to those of the bare soil, since both the air entry value, as well as the slope of curve between the air entry value and the water entry value result to be lower.

Furthermore, the coefficient of saturated permeability, k_{sat}, was found to be highly sensitive to the presence and density of roots. By means of different techniques, *i.e.,* in-situ and laboratory testing, as well as numerical modelling, it was recognized that roots tend to increase the coefficient of saturated permeability. The impact of roots on the soil properties may appear not beneficial for the stability of slopes; however, it is worth mentioning that the vegetation layer also induce relevant water interception, which in turn makes lower net water fluxes across the ground level.

Finally, it was also presented an equation to predict the value of the k_{sat} for rooted soil, which is believed to be of quantitative use for the Pisciolo slope here of reference, but it may hold only a qualitative significance with reference to different materials and case studies.

However, in this work some issues were not addressed and will be the object of further research; experimental studies have to be performed to determine the REV of the soil-root composite; also a bio-chemical study needs to be carried out since it has been recognized that the root system may impact strongly the chemistry of the soil pore water.

Acknowledgements

The authors are grateful for the financial support provided by MIUR PON R&I 2014-2020 program (project MITIGO, ARS01_00964) and project PNRR, MISURA M4_C2_1.4, National Centre for HPC, Big Data and Quantum Computing (CN_00000013) - Spoke 5 “Environments and Natural Disasters”.

References

Apollonio C, Petroselli A, Tauro F, Cecconi M, Biscarini C, Zarotti C, Grimaldi S. Hillslope erosion mitigation: An experimental proof of a nature-based solution. *Sustainability*. 2021 May 27;13(11):6058. https://doi.org/10.3390/su13116058

Assadi-Langroudi A, O’Kelly BC, Barreto D, Cotecchia F, Dicks H, Ekinci A, Garcia FE, Harbottle M, Tagarelli V, Jefferson I, Maghoul P. Recent advances in nature-inspired solutions for ground engineering (NiSE). International *Journal of Geosynthetics and Ground Engineering*. 2022 Feb;8(1):3. https://doi.org/10.1007/s40891-021-00349-9

Avci CB. Analysis of in situ permeability tests in nonpenetrating wells. *Groundwater*. 1994 Mar;32(2):312-22. https://doi.org/10.1111/j.1745-6584.1994.tb00646.x

Benjamin JG, Nielsen DC. A method to separate plant roots from soil and analyze root surface area. *Plant and Soil*. 2004 Dec;267:225-34. http://doi.org/ 10.1007/S11104-005-4887-3

Bentley, “Plaxis Manuals, 2022.” https://communities.bentley.com/products/geotech-analysis/w/wiki/46137/manuals---plaxis

Biot MA. General theory of three-dimensional consolidation. *Journal of applied physics*. 1941 Feb;12(2):155-64. http://doi.org/10.1063/1.1712886

Bishop AW. The principle of effective stress. *Teknisk ukeblad*. 1959;39:859-63.

Blight GE. Interactions between the atmosphere and the earth. *Géotechnique*. 1997;47(4):715-67. https://doi.org/10.1680/geot.1997.47.4.713

Bottiglieri O, Cafaro F, Cotecchia F. Estimating the retention curve of a compacted soil through different testing and interpretation methods. *InUnsaturated Soils: Research and Applications*: Volume 1 2012 (47-54). Springer Berlin. https://doi.org/10.1007/978-3-642-31116-1

Chandler, R. J., Leroueil, S. and Trenter, N. A., Measurements of the Permeability of London Clay Using a Self-Boring Permeameter, vol. 40, no. 1, pp. 113–24. https://Doi.Org/10.1680/Geot.1990.40.1.113

Chapuis RP. Shape factors for permeability tests in boreholes and piezometers. *Groundwater*. 1989 Sep;27(5):647-54. https://doi.org/10.1111/j.1745-6584.1989.tb00478.x

Childs EC, Collis-George N, Holmes JW. Permeability measurements in the field as an assessment of anisotropy and structure development. *Journal of Soil Science*. 1957 Mar;8(1):27-41. https://doi.org/10.1111/j.1365-2389.1957.tb01865.x

Cotecchia, F., Pedone, G., Bottiglieri, O., Santaloia, F., and Vitone, C., Slope-Atmosphere Interaction in a Tectonized Clayey Slope: A Case Study, *Italian Geotechnical Journal*, 2014.

Cotecchia, F., Tagarelli, V., Pedone, G., Ruggieri, G., Guglielmi, S. and Santaloia, F., Analysis of Climate-Driven Processes in Clayey Slopes for Early Warning System Design, vol. 172, no. 6, pp. 465–80. https://Doi.Org/10.1680/Jgeen.18.00217

Cui Y, Zhang YH, Zhou SJ, Pan YY, Wang RQ, Li Z, Zhang ZM, Zhang MX. Cracks and root channels promote both static and dynamic vertical hydrological connectivity in the Yellow River Delta. *Journal of Cleaner Production*. 2022 Sep 20;367:132972. https://doi.org/10.1016/j.jclepro.2022.132972

Di Lernia, A., Cotecchia, F., Elia, G., Tagarelli, V., Santaloia, F. and Palladino, G., Assessing the Influence of the Hydraulic Boundary Conditions on Clay Slope Stability: The Fontana Monte Case Study, *Engineering Geology*, vol. 297, 2022. http://doi.org/10.1016/J.ENGGEO.2021.106509

Elia, G., Cotecchia, F., Pedone, G., Vaunat, J., Vardon, P. J., Pereira, C., Springman, S. M., et al., Numerical Modelling of Slope-Vegetation-Atmosphere Interaction: An Overview, Quarterly *Journal of Engineering Geology and Hydrogeology*, vol. 50, no. 3, pp. 249–70, August 1, 2017. https://doi.org/10.1144/qjegh2016-079

Elrick, D. E., Reynolds, W. D. and Tan, K. A., Hydraulic Conductivity Measurements in the Unsaturated Zone Using Improved Well Analyses, *Groundwater Monitoring & Remediation*, vol. 9, no. 3, pp. 184–93, June 1, 1989. http://doi.org/10.1111/J.1745-6592.1989.TB01162.X

Fraccica A, Romero Morales EE, Fourcaud T. Multi-scale effects on the hydraulic behaviour of a root-permeated and compacted soil. In *IS-Glasgow 2019–7th International Symposium on Deformation Characteristics of Geomaterials* (pp. 1-5). EDP Sciences.

Galavi, V., Groundwater Flow, Fully Coupled Flow Deformation and Undrained Analyses in PLAXIS 2D and 3D - Wiki - GeoStudio PLAXIS - Bentley, 2010.

Gens A. Soil–environment interactions in geotechnical engineering. *Géotechnique*. 2010 Jan;60(1):3-74.. https://Doi.Org/10.1680/Geot.9.P.109

Genuchten, M., Leij, F. and Yates, S., The RETC Code for Quantifying the Hydraulic Functions of Unsaturated Soils, 1992.

Genuchten, M. Th. van, A Closed-Form Equation for Predicting the Hydraulic Conductivity of Unsaturated Soils, *Soil Science Society of America Journal*, vol. 44, no. 5, pp. 892–98, 1980. http://doi.org/10.2136/SSSAJ1980.03615995004400050002X

Leroueil, S., Natural Slopes and Cuts: Movement and Failure Mechanisms, *Geotechnique*, vol. 51, no. 3, pp. 197–243, 2001. https://doi.org/10.1680/geot.2001.51.3.197

Lu, J., Zhang, Q., Werner, A. D., Li, Y., Jiang, S. and Tan, Z., Root-Induced Changes of Soil Hydraulic Properties – A Review, *Journal of Hydrology*, vol. 589, p. 125203, 2020. https://doi.org/10.1016/j.jhydrol.2020.125203

Marinho, F. A. M. and Oliveira, O. M., The Filter Paper Method Revisited, *Geotechnical Testing Journal*, vol. 29, no. 3, pp. 250–58, 2006. http://doi.org/10.1520/GTJ14125

Mualem, Y., A New Model for Predicting the Hydraulic Conductivity of Unsaturated Porous Media, *Water Resources Research*, vol. 12, no. 3, pp. 513–22, 1976. http://doi.org/10.1029/WR012I003P00513

Pedone G, Tsiampousi A, Cotecchia F, Zdravkovic L. Coupled hydro-mechanical modelling of soil–vegetation–atmosphere interaction in natural clay slopes. *Canadian Geotechnical Journal*. 2022;59(2):272-90. http://doi.org/10.1139/CGJ-2020-0479

Pedone G, Cotecchia F, Tagarelli V, Bottiglieri O, Murthy MB. An Investigation into the Water Retention Behaviour of an Unsaturated Natural Fissured Clay. *Applied Sciences*. 2022 Sep 22;12(19):9533. https://doi.org/10.3390/app12199533

Pirone, M., Papa, R., Nicotera, M. V. and Urciuoli, G., In Situ Monitoring of the Groundwater Field in an Unsaturated Pyroclastic Slope for Slope Stability Evaluation, *Landslides*, vol. 12, no. 2, pp. 259–76, 2015. https://doi.org/10.1007/s10346-014-0483-z

Reynolds, W. D., and Elrich, D. E., In Situ Measurement of Field-Saturated Hydraulic Conductivity, Sorptivity, and the Alpha-Parameter Using the Guelph Permeameter, *Soil science*, 1985.

Seethepalli, A., Dhakal, K., Griffiths, M., Guo, H., Freschet, G. T. and York, L. M., RhizoVision Explorer: Open-Source Software for Root Image Analysis and Measurement Standardization, *AoB PLANTS*, vol. 13, no. 6, 2021. http://doi.org/10.1093/AOBPLA/PLAB056

Shackelford, C. D., Javed, F., Shackelford, R. : and Javed, C. D., Large-Scale Laboratory Permeability Testing of a Compacted Clay Soil, *Engr.Colostate*.Edu, vol. 14, no. 2, pp. 171–79, 1991. http://doi.org/10.1520/GTJ10559J

Smethurst JA, Clarke D, Powrie W. Factors controlling the seasonal variation in soil water content and pore water pressures within a lightly vegetated clay slope. *Géotechnique*. 2012 May;62(5):429-46. https://doi.org/10.1680/geot.10.P.097

Soilmoisture Equipment Corp., Guelph permeameter kit, 2008.

Tagarelli, V. and Cotecchia, F., Deep Movements in Clayey Slopes Relating to Climate: Modeling for Early Warning System Design, *Lecture Notes in Civil Engineering*, vol. 40, pp. 205–14, 2019. http://doi.org/10.1007/978-3-030-21359-6_22

Tagarelli, V. and Cotecchia, F., Preliminary Field Data of Selected Deep-Rooted Vegetation Effects on the Slope-Vegetation-Atmosphere Interaction: Results from an in-Situ Test, *Italian Geotechnical Journal*, vol. 56, no. 1, pp. 62–83, 1/1, 2022. http://doi.org/10.19199/2022.1.0557-1405.062

Tagarelli, V. and Cotecchia, F., The Effects of Slope Initialization on the Numerical Model Predictions of the Slope-Vegetation-Atmosphere Interaction, *Geosciences* 2020, Vol. 10, Page 85, vol. 10, no. 2, p. 85, 2020. https://doi.org/10.3390/geosciences10020085

Tagarelli V, Cotecchia F. Coupled hydro-mechanical analysis of the effects of medium depth drainage trenches mitigating deep landslide activity. *Engineering Geology*. 2022 Feb 1;297:106510. https://doi.org/10.1016/j.enggeo.2021.106510

Toll, D. G., Lourenço, S. D. N., Mendes, J., Gallipoli, D., Evans, F. D., Augarde, C. E., Cui, Y. J., et al., Soil Suction Monitoring for Landslides and Slopes, *Quarterly Journal of Engineering Geology and Hydrogeology*, vol. 44, no. 1, pp. 1–13, 2011. http://doi.org/10.1144/1470-9236/09-010

Vergani, C. and Graf, F., Soil Permeability, Aggregate Stability and Root Growth: A Pot Experiment from a Soil Bioengineering Perspective, *Ecohydrology*, vol. 9, no. 5, pp. 830–42, 2016. http://doi.org/10.1002/ECO.1686

Wu, G.-L., López-Vicente, M., Huang, Z., Cui, Z., and Liu, Y.: Preferential water flow through decayed root channels enhances soil water infiltration: Evaluation in distinct vegetation types under semi-arid conditions, *Hydrol. Earth Syst. Sci. Discuss.*, https://doi.org/10.5194/hess-2020-266, 2020